ARTICLES

Ultrafast Solvation Dynamics: A View from the Solvent's Perspective Using a Novel Resonant-Pump, Nonresonant-Probe Technique

David F. Underwood and David A. Blank*

Department of Chemistry, University of Minnesota, 207 Pleasant Street SE, Minneapolis, Minnesota 55455

Received: October 4, 2002; In Final Form: December 12, 2002

The condensed-phase solvation dynamics of those molecules in immediate proximity to an excited-state chromophore were probed with femtosecond time resolution by a technique that employs resonant optical excitation of the chromophore followed by a nonresonant third-order Raman probe of the solvent. This new method provides a microscopic perspective from the point of view of those solvent molecules that make up the local environment of a dynamic event. In this initial study, we have investigated the solvation dynamics of 9,10-diphenylanthracene dissolved in chloroform.

Introduction

The role of the solvent in condensed-phase chemical reactions is of pivotal importance, from determining reaction rates in simple transformations to understanding the complex behavior of proteins in their liquid environment. The majority of the measurements aimed at collecting a solvent response have either been performed on neat solvents[1−6] or have done so through a reporter chromophore.[7−13] The interpretation of the solvent response through coupling to a reporter chromophore can offer a limited picture of the dynamics, particularly in nondipolar solvation where the coupling becomes weak, and the response is often dominated by the intramolecular motions of the chromophore itself.[14−16] Furthermore, reliance on a reporter will most often preclude application to reactive systems, where the reactive event itself can dominate any change in the spectral characteristics of the reporter, effectively blinding the experiment to the response of the surrounding solvent.

Motivated by the desire to decouple the measurement of the solvent response from any additional solute dynamics, we have procured a direct measurement of the response of a solvent reacting to the resonant excitation of a chromophore, with 36 fs resolution in the time domain. While the use of time-domain nonresonant third-order Raman (TOR) spectroscopy has reached a mature level of development in probing the response of neat liquids,[1−6,17−20] to our knowledge TOR spectroscopy has not been used as a *probe* following an electronically resonant photoinitiated process such as solvation. Applicable to practically any condensed-phase system, the ability to directly probe the response of the solvent molecules with nonresonant spectroscopy will offer a near limitless range of dynamic events that one can observe from the perspective of the molecular environment local to the event.

While offering complementary information to experiments that utilize a resonant probe in the THz region of the spectrum,[21,22] the time-domain nonresonant TOR probe has some advantages: (1) A greater time resolution is offered by the shorter laser pulses that are readily generated in the visible and near-IR portion of the spectrum. The time resolution of the experiment related to the dynamical event is dictated by the laser pulse width, in this case 36 fs. (2) A broader spectral region of the molecular motions are covered in a single scan, currently 0.1−500 cm^{-1}. This is determined at the high-frequency end by the width of our laser pulses in time and at the low-frequency end by the overall length of the scan in time. (3) The nonresonant probe prevents difficulties associated with samples that are nearly optically opaque, even over extremely short path lengths. (4) The tensoral nature of the response allows the separation of the electronic and nuclear components[23] and allows the separation of nuclear motions based on symmetry.[24,25]

Here we describe the initial implementation of this new approach with a study of the response of chloroform to an electronically resonant, optical excitation of the solute 9,10-diphenylanthracene (9,10-DPA). This chromophore has no dipole moment in either the ground or the excited state but does possess a significant quadrupole moment that changes upon excitation.[26] As a result, the solvation dynamics in this system lie somewhere between purely dipolar and purely nondipolar. Unlike the purely dipolar counterparts where models of the solvation dynamics have reached an advanced level of development,[27−32] the dipolar-solvent−quadrupolar-solute situation has received far less attention. The short-range, weaker interactions in the present case offer an indication of the sensitivity and range of dynamics that can be studied with this technique.

Indeed, in this case we corroborate the expected ultrafast component of the solvation and quantify a 190 fs peak in the response after the electronic excitation of the chromophore. Following the ultrafast response, we are able to monitor the subsequent transition to the "steady-state" solvation of 9,10-DPA in its long-lived electronic excited state. The experiments carry an additional piece of information with the time-domain dynamics in that we are able to relate the absolute sign of the response to the change in the polarizability of the adjacent

* E-mail: blank@chem.umn.edu. Phone: (612) 624-0571. Fax: (612) 624-1589.

10.1021/jp027134e CCC: $25.00
Published on Web 01/22/2003

molecular environment. These data indicate an initial ultrafast increase in the change in the solvent polarizability in conjunction with the inertial response, followed by a decrease in the polarizability change that falls negative during the extended time scales of solvation.

Experimental Section

Generation of Ultrafast Laser Pulses. The ultrafast laser pulses used in these experiments were generated in a home-built titanium:sapphire oscillator/amplifier system based on previous works;[33] we include the following description for completeness. The Kerr lens mode-locked oscillator was built in a standard X-geometry configuration with a 3 mm diameter × 4 mm path length (Ti 0.25%) Ti:sapphire rod (Bicron), pumped with 3.5 W from a continuous-wave Nd:yttrium lithium fluoride (YLF) laser (Millenia, Spectra-Physics, Inc.). The average output power was 400 mW, and intracavity dispersion compensation with a fused silica prism pair led to a p-polarized output bandwidth of 60 nm [full width at half-maximum (fwhm)]. The oscillator pulses were stretched in an all-reflective stretcher−compressor (Kapteyn-Murnane Labs, Inc.) to approximately 100 ps.

The stretched pulses were introduced into the regenerative amplifier (regen) by passing them through a polarizing beam-splitter cube (CVI) and subsequently s-polarized by means of a quartz Faraday rotator (Optics for Research, Inc.). The vertically polarized pulses were directed into the cavity of the regen using a thin-film polarizer, and a Pockels cell (Thomson-CSF, with pre-bias option) controlled the timing of the pulse entry. The injected pulses made, on average, nine round trips in a V-shaped cavity and were then ejected by the Pockels cell into a two-pass amplifier. Both the regen and the two-pass amplifier were pumped with a Q-switched Nd:YLF laser (Evolution-30, Positive Light, Inc.) triggered at a repetition rate of 1 kHz, which was timed from the 88 MHz oscillator pulse train (the regen and two-pass amplifier were pumped with 5.0 and 12 W, respectively). The pump beam for the regen was expanded to approximately 2.0 in. using a lens pair (BE in Figure 1) prior to focusing through mirror CM1 to the 3 × 5 mm (0.25% Ti) Ti:sapphire rod. The distance between the curved mirrors CM1 and CM2 was 1 m, and a second curved mirror (CM3) served to refocus the portion of the 527 nm light that leaked through CM2 back to the Ti:sapphire crystal. The same method was used in the two-pass amplifier using curved mirror CM6. The distance between CM4 and CM5 is 0.5 m, and the 5 × 5 mm (Ti 0.25%) Ti:sapphire crystal was placed outside the focus, closer to CM4. The amplified pulses were compressed to 36 fs (intensity, fwhm), measured by standard three-pulse transient grating (TG) and three-pulse TG-frequency-resolved optical gating[34,35] through a quartz window at the location of the sample cell.

Pulse energies of 2.5 mJ are attainable when required; for the current investigation, the system was set to produce 1.5 mJ per pulse. A portion of the output was split using a waveplate/polarizing beamsplitter cube pair, with the p-polarized portion directed through a 1 mm β-BaB_2O_4 (BBO) crystal (CXK Optronics) for type I frequency doubling without focusing. The 400 nm beam was compressed to 35 fs using a pair of equilateral fused silica prisms. Both the 800 and the 400 nm beams were collimated to 3 mm in diameter using fused silica lens sets before reaching the experimental portion of the table.

Resonant-Pump, Third-Order Raman Spectroscopy (RaPTORS). The experiment proceeds as follows: a variably delayed resonant excitation "pump" pulse (400 nm) excites the chromophore in solution, thus initiating the solvation action of the solvent. 9,10-DPA has a strong absorption at 400 nm, undergoing an $S_0 \rightarrow S_1$ transition,[36] while chloroform is transparent at this wavelength with negligible two-photon absorption.[37] The response of the solvent is then probed by nonresonant TOR spectroscopy using the 800 nm pulses. A lock-in amplifier detects the modulation in the signal produced by the presence of the 400 nm pulse. The pulse sequence for the RaPTORS technique is shown in Figure 2.

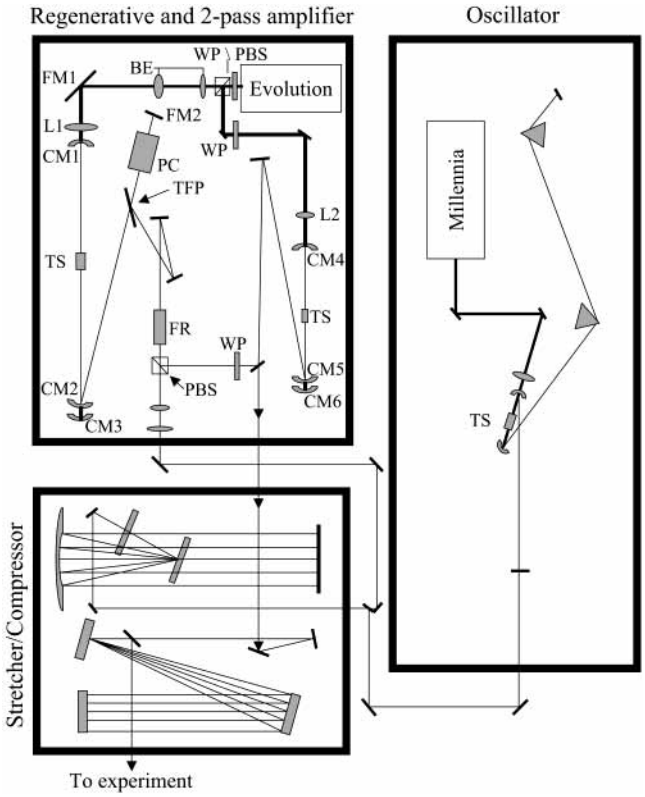

Figure 1. Schematic of the ultrafast laser system used in this study. Legend: PBS, polarizing beam splitter; WP, waveplate; BE, beam expander; L, lens; FM, flat mirror; CM, curved mirror; TS, Ti/sapphire crystal; PC, Pockels cell; TFP, thin-film polarizer; FR, Faraday rotator.

The TOR probe was set up in a standard box geometry. A pair of horizontally displaced 800 nm pulses were mechanically timed relative to each other, time delay τ, and focused onto a 1 mm thick fused silica diffractive optic (MEMS Optical) using a 1 m radius of curvature silver mirror, where they were vertically diffracted into their multiple orders. A 0.5 m radius of curvature mirror imaged the diffractive optic onto the sample area. A mask was used to select only the +1 and −1 diffraction orders from pulse one, providing the time-coincident interaction pair E_1 and E_2. The +1 diffraction order from pulse two provided E_3 (see Figure 2).[19,20] The 400 nm excitation pulse traversed an optical delay after compression and copropagated between the two 800 nm beams; following the diffractive optic, the zero-order diffraction was used to excite the sample, so the 400 nm pulse travelled down the center of the TG "box". The arrival of the 400 nm pulse at the sample is defined as $t = 0$, and the arrival of the time-coincident nonresonant pair, E_1 and E_2, is defined as $\tau = 0$.

All four pulses were focused to a quartz sample flow cell (1 mm path length, Starna Cells, #48-Q-1) in which the sample solution flowed at a rate of about 0.1 mL/s. The RaPTOR signal was collected along the unique direction defined by the phase matching condition for E_1, E_2, and E_3.[38] The signal was polarization-selected, passed through a narrow band-pass filter

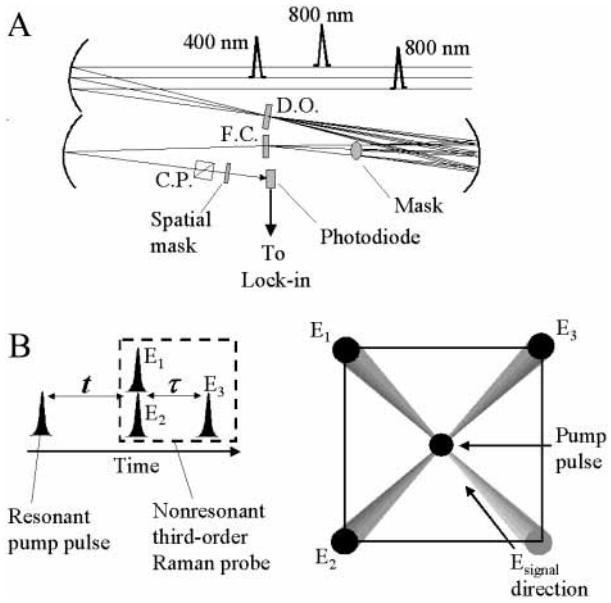

Figure 2. (A) Schematic diagram of the experiment. The three incoming beams are focused to a diffractive optic (D.O.) using a 1.0 m focal length (fl) silver mirror. The focus is imaged with a 0.5 m fl mirror to the flow cell; a mask blocks all but the three 800 nm beams in the "box" configuration and allows the 400 nm resonant pulse to propagate down the center (normal to the sample cell). The RaPTOR signal is focused using another 0.5 m fl silver mirror through a cube polarizer (C.P.) to a photodiode. (B) Timing sequence for the RaPTORS experiment (left) and three-dimensional depiction (viewing normal to the flow cell) of the incoming laser fields (right).

centered at 800 nm, and focused onto a fast silicon photodiode (Thor-Labs DET210). Finally, the signal was sent to a lock-in amplifier (SR810, Stanford Research), digitized, and stored on a personal computer.

Suppression of the electronic components to the TOR probe signal was accomplished using polarization selection, as described previously.[23,24] For all of the data herein, the polarization of pulse E_3 was set to $+45°$ from pulses E_1 and E_2 and the pump pulse, which were all set to vertical using waveplate/polarizing beamsplitter cubes in each arm. The signal polarization was filtered using a polarizing beamsplitter cube set to $-71°$ from the vertical to suppress the electronic contribution.

The 400 nm pump beam was mechanically chopped at a frequency of 500 Hz; therefore, the lock-in amplifier detected the *change* in the TOR response as a result of excitation of the chromophore, as discussed below. No signal was detected in the absence of 9,10-DPA (i.e., neat solutions of chloroform) in the RaPTOR configuration, and the same was true when each of the four incoming beams was blocked independently with 9,10-DPA present. By altering the incoming angle of the pump beam through vertical displacement in the RaPTORS geometry, we determined that the RaPTOR signal was insensitive to the propagation direction of the incoming 400 nm pump beam.

The power dependence of the signal was shown to behave linearly with each of the four participating beams; therefore, we rule out multiphoton absorption and higher-order effects. The chromophore concentration for the data presented here was 0.5 mM, with an optical density of 0.4 at 400 nm.

Results

In the absence of the resonant pump pulse, the TOR probe signal is identical to that of the neat solvent. This is a result of the nonresonant nature of the probe interactions that leave the response dominated by the bulk solvent. The homodyne-detected

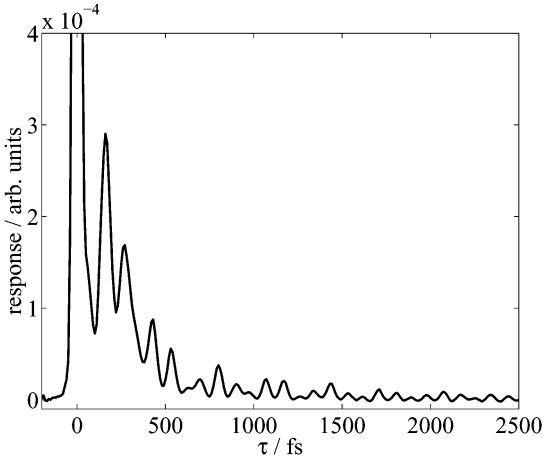

Figure 3. Homodyne-detected electronically nonresonant TG response of 0.5 mM 9,10-DPA in chloroform. Within the quality of our data, this response was found to be identical to that of neat chloroform.

TOR signal is proportional to the modulus-squared emitted signal field, which is proportional to the polarization created by the three nonresonant probe fields,

$$I_{\text{no pump}}(\tau) \propto |E^{(3)}_{\text{solvent}}(\tau)|^2 \propto |P^{(3)}(\tau)|^2 \qquad (1)$$

The one-dimensional homodyne-detected TG response is shown in Figure 3. In addition to the overdamped intermolecular response, beats from the ν_6 and ν_3 intramolecular modes in chloroform (identified via Fourier transform) are clearly evident.

In the TOR response, the time-domain dynamics are contained in the polarizability correlation function,[38]

$$R^{(3)}(t') = -(i/\hbar)\langle[\alpha(t'), \alpha(0)]\rho(-\infty)\rangle \qquad (2)$$

and the polarization, $P^{(3)}(\tau)$, can be expressed as the integral of the third-order response function over the time delay between nonresonant field-matter interactions, t'. Given finite laser pulse widths, a final convolution over the pulse envelopes is required to quantitatively relate the signal to $P^{(3)}(\tau)$.[6,38]

When the pump pulse is present, there is a small change in the TOR signal field, $\Delta E^{(3)}(t,\tau)$, reflecting the response of the system to the resonant excitation of the solute:

$$I_{\text{pump present}}(t,\tau) \propto |E^{(3)}_{\text{solvent}}(\tau) + \Delta E^{(3)}(t,\tau)|^2 \qquad (3)$$

The RaPTORS experiment measures the difference between the signals when the pump pulse is present, eq 3, versus absent, eq 1. Under the assumption that $\Delta E^{(3)}(t,\tau) \ll E^{(3)}_{\text{solvent}}(\tau)$, the measured signal is proportional to the cross term,

$$I_{\text{RaPTOR}}(t,\tau) \propto \Delta E^{(3)}(t,\tau)\, E^{(3)}_{\text{solvent}}(\tau) \qquad (4)$$

The one-dimensional solvent response, $E^{(3)}_{\text{solvent}}(\tau)$, acts as an intrinsic local oscillator for heterodyne detection of the desired two-dimensional signal, $\Delta E^{(3)}(t,\tau)$. This is advantageous because it offers amplification, recovery of sign, and phase selection of the two-dimensional signal. The phase selection reflects the fact that the probe pulses are electronically nonresonant, leaving the intrinsic local oscillator to be dominated by the real component of the complex signal field.[39] Although one must be cautious to remember that the data reflect the inclusion of a time-dependent local oscillator along the τ time dimension, the clear evolution of the signals along both time dimensions demonstrates that we are probing the desired two-dimensional response.

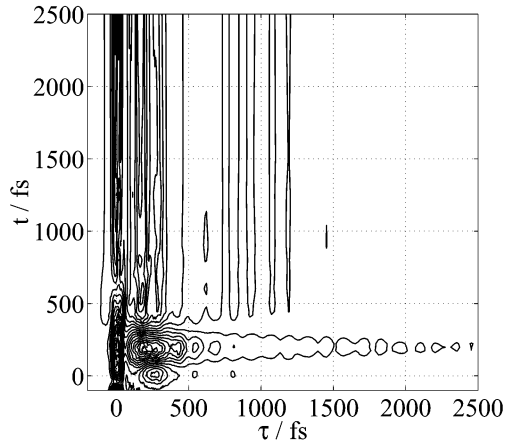

Figure 4. Two-dimensional RaPTOR spectrum of 9,10-DPA in chloroform. Note that the values are positive for $0 < t < 325$ fs and negative for $t > 325$ fs (see Figures 5 and 6).

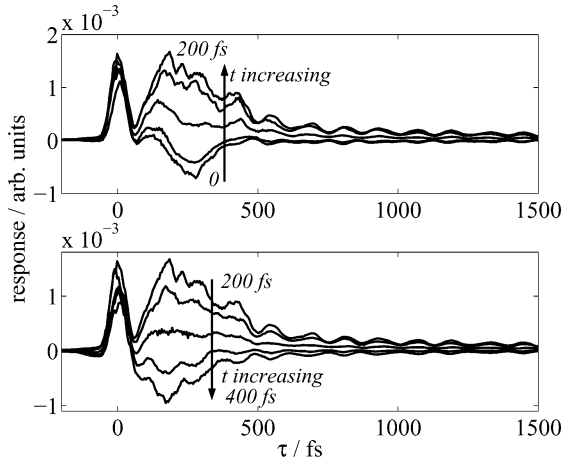

Figure 5. Slices along the τ axis for time values of t following the resonant pulse from the data in Figure 4. Slices intersect the timeline toward increasing t. Top: $t = 0$, 50, 100, 150, and 200 fs. Bottom: $t = 200$, 250, 300, 350, and 400 fs.

In addition, the measured cross term is finite only for nonzero values of $\Delta E^{(3)}(t,\tau)$, confirming that the signal must reflect the two-dimensional response. Recovering $\Delta E^{(3)}(t,\tau)$ alone requires division of the detected signal by the time-dependent local oscillator, which in turn requires measurements of both the RaPTOR signal and $E^{(3)}_{\text{solvent}}(\tau)$ under identical conditions. These experiments are currently underway in our laboratory employing a time-*in*dependent local oscillator for the determination of $E^{(3)}_{\text{solvent}}(\tau)$.[18−20]

Figure 4 shows the two-dimensional RaPTOR spectrum for 9,10-DPA in chloroform with the laser polarizations set to enhance the nuclear portion of the response.[23] Slices from the two-dimensional data set along the τ dimension for a given delay t from the excitation pulse illustrate how the RaPTOR technique affords a method to watch the inter- and intramolecular frequencies evolve in time after the initial photoexcitation (Figure 5). The sharp signal at $\tau = 0$ is the electronic response of the chloroform, which is present due to a small amount of polarizer leakage; however, the characteristic nuclear beating pattern is fully evident past this feature and extends for several picoseconds.

Focusing on the early time dynamics, we notice a growth in the RaPTOR signal for $t = 0-190$ fs, followed by a gradual decrease and then a change in the signal sign for $t > 325$ fs. In addition, distinct changes in the beating pattern along τ are

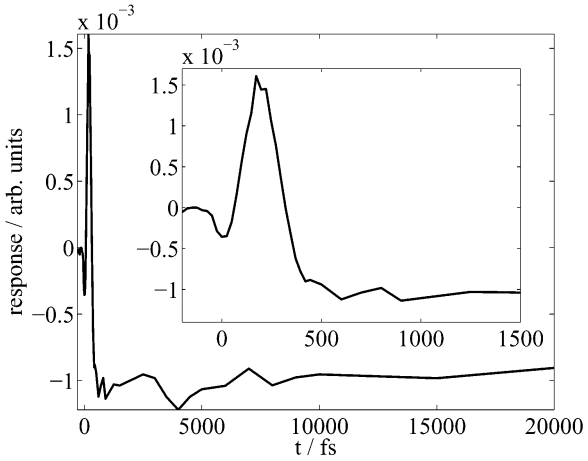

Figure 6. Slice along t for $\tau = 200$ fs from the data in Figure 4; the inset shows the early dynamics in higher resolution.

evident as the system evolves from $t = 0$. A one-dimensional slice along t at $\tau = 200$ fs shows the progression of the signal with the aforementioned properties (Figure 6). It is important to note that, when looking at a slice along the t dimension for a fixed value of τ, the local oscillator becomes time-*independent*, leaving the dynamics completely dictated by the $\Delta E^{(3)}(t,\tau)$ term in eq 4. Farther out along t, the RaPTOR signal is almost as intense at $t = 20$ ps as it is at $t = 1$ ps (Figure 6). Beyond $t = 1$ ps there is a weak decay component with a time scale of about 4 ps and a dominant component with a very long time scale, appearing nearly constant within the 20 ps of our measurement. The long time scale is consistent with the reported excited-state lifetime of 9,10-DPA.[40] An experimental limitation with the length of our stage travel prevents the quantification of this roughly 10 ns decay.

Discussion

The signal field from the third-order nonresonant probe in our experiments reflects the polarizability of our many-body system in the form of a single-time two-point correlation function, eq 2. The RaPTOR signal is a measure of the change in that polarizability, reflected by $\Delta E^{(3)}(t,\tau)$ in eq 4, in dynamic response to the excitation of the 9,10-DPA chromophore.

It follows that a positive signal indicates a situation in which the probed molecules are more polarizable than those of the solvent in equilibrium and vice versa. Presumably, the first motions of solvation for this weakly polar system would include the inertial component as the chloroform molecules align their dipole moments in response to the change in the electronic configuration of the chromophore. As evidenced in Figure 6, these dynamics initially show an increase in the polarizability that peaks at $t = 190$ fs, reflecting the point of maximum inertia accumulated by the reorganizing solvent molecules. From $t = 190$ to 600 fs there is a rapid decline, with the signal changing sign from positive to negative at 325 fs. As the solvent equilibrates around the excited chromophore, it becomes less polarizable and the RaPTOR signal becomes negative. This reduction in the polarizability of the intermolecular nuclear motions reflects a tightening of the intermolecular potential between solvent and solute upon electronic excitation of the solute.

The 200 fs ultrafast response in the RaPTOR signals in Figure 6 agrees well with typical inertial time scales of solvent reorientation.[9,27] Using fluorescence upconversion on the dipolar system of Coumarin 153 in chloroform, Maroncelli and co-

workers have reported a time scale of 285 fs for the inertial component.[9] Considering that it is not the peak of the response that should be compared directly with the exponential time scale from the time-resolved fluorescence measurements, but the overall time scale of the inertial response, the agreement between the experiments is reasonable.

While the similarity in ultrafast time scales is consistent with the idea that we are seeing the same type of electrostatically driven response from the solvent to a quadrupolar change in 9,10-DPA that Maroncelli and co-workers saw with a dipolar change in Coumarin 153, it is not sufficient to conclude that our response is the inertial realignment of the solvent's dipolar orientation alone. Maroncelli and co-workers have shown that a similar electrostatically driven response is found when looking at dipolar solutes in nondipolar solvents;[41] however, Berg has demonstrated that in nondipolar solvent−solute systems a similar time scale can be explained by the response of the system to the ballistic expansion or contraction of the chromophore upon excitation.[14] Using a photon echo technique, Larsen et al. have observed very similar 100 fs time scales in both dipolar and nondipolar solvents using a nondipolar solute as a solvation probe.[16]

We expect to be able to further address the separation of ultrafast dipolar and nondipolar response components in future experiments by taking advantage of the tensoral nature of the RaPTOR response. The inertial dipolar response will be highly anisotropic while the nondipolar response proposed by Berg should be more isotropic, particularly in the case of a symmetric solute molecule. By selecting the appropriate relative polarizations of the three nonresonant probe fields in the RaPTOR experiment, we can probe the isotropic and anisotropic solvent responses independently.[25]

Following the initial ultrafast response, the signal in Figure 6 decays back toward zero with two discernible components. The slow component has a large amplitude, and the decay rate is almost imperceptible on the 20 ps time scale of our experiment. We assign this recovery to the relaxation of the electronically excited 9,10-DPA chromophores, which have an approximately 10 ns excited-state lifetime.[40] The faster decay has a very small amplitude and a time scale of about 4 ps. We attribute this relaxation time scale to intermediate solvent reorganization. In the dipolar Coumarin−chloroform system, Maroncelli and co-workers reported a 4.15 ps decay component with twice the amplitude of the ultrafast response.[9] While the dipolar Coumarin system might be expected to exhibit different ultrafast dynamics on the basis of the substantial difference in the solvent−solute interaction, the intermediate reorganization of the solvent will be more strongly influenced by the solvent−solvent interactions, providing a limited foundation for the comparison of the intermediate time scale between the two experiments.

In contrast to that for the dipolar Coumarin system, our measurement shows the overall magnitude of the dynamics dominated by the ultrafast component. Castner and Maroncelli have discussed the comparison between resonant and nonresonant (TOR) probes of solvation dynamics.[42] They demonstrated that when comparing the raw data, the relative weighting of the impulsive to intermediate solvation components is larger in the case of a nonresonant probe. However, this difference in the relative sensitivities of the two techniques does not appear to be enough to explain the very large difference in the measured magnitude of the two components. While the time scale of the intermediate response is found to be the same when using the same solvent, the more subtle quadrupolar change in 9,10-DPA

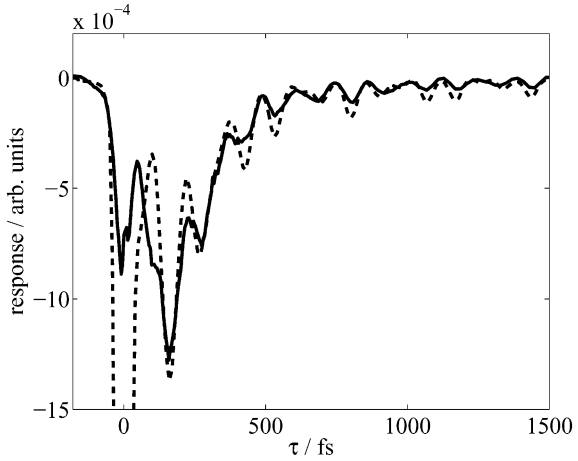

Figure 7. Comparison of the homodyne-detected solvent TG and the RaPTOR signal at long pump delay. Solid line: RaPTOR signal along τ for $t = 20\,000$ fs. Dashed line: Homodyne-detected TG shown in Figure 3 multiplied by 4.7 and inverted for comparison.

appears to reduce the amplitude of the intermediate response relative to the ultrafast component. A possible explanation for the reduced amplitude in the intermediate response could be the relatively weaker and shorter range of the quadrupole−dipole interaction. Future experiments will simultaneously measure the RaPTOR signal and $E^{(3)}_{\text{solvent}}(\tau)$, allowing the removal of the local oscillator from the RaPTOR surface and recovery of $\Delta E^{(3)}(t_{\text{fixed}},\tau)$ alone. Such measurements will allow for direct comparisons of the amplitudes of different solvation components between our experiments and resonant solvation probes as outlined by Castner and Maroncelli.[42]

At large values of t, we can compare the response of the solvent equilibrated in the local environment of an electronically excited 9,10-DPA molecule with that of the bulk solvent. Figure 7 compares a slice of the RaPTOR response along τ at $t = 20$ ps and the TG response of the solvent in the absence of the resonant pump pulse. Note that the bulk solvent response from Figure 3 has been inverted and scaled for comparison, arbitrarily making the overdamped portion of both responses appear with equal intensity. From eq 4, the RaPTOR signal for a fixed value of t is proportional to the product of the change induced by the excitation of the chromophore and the electric field of the nonresonant response from the bulk solvent $[\Delta E^{(3)}(t_{\text{fixed}},\tau)\, E^{(3)}_{\text{solvent}}(\tau)]$. In Figure 7, we are comparing this to the homodyne-detected TG response, which is the product of the electric field of the nonresonant response from the bulk solvent and its complex conjugate, eq 1 $[[E^{(3)}_{\text{solvent}}(\tau)]^* E^{(3)}_{\text{solvent}}(\tau)]$. The overdamped responses in both measurements are very similar. This suggests that the response of the bulk solvent to the perturbation from the nonresonant laser fields is nearly identical to the change in polarizability of the local solvent when going from equilibrated around the ground state 9,10-DPA to equilibrated around the electronically excited 9,10-DPA [reflected in $\Delta E^{(3)}(t_{\text{fixed}},\tau)$]. This result offers direct, albeit limited, support for the common assumption of linear response when considering the intermolecular motions in solution.

It is notable that the ratio of the intramolecular response, as reflected in the high-frequency beating patterns, to the overdamped intermolecular response is different in the two measurements shown in Figure 7. The RaPTOR signal shows a relatively smaller intramolecular response. This demonstrates that the change in the local field when exciting the 9,10-DPA chromophore results in a (relatively) smaller change in the polarizability of the intramolecular vibrations of the solvent molecules

than that induced by the impulsive excitation of the nonresonant laser fields. Future experiments providing removal of the local oscillator from the RaPTOR signal will allow a direct comparison of $\Delta E^{(3)}(t_{\text{fixed}},\tau)$ and $E^{(3)}_{\text{solvent}}(\tau)$ and quantification of this difference.

Conclusion

We have demonstrated the ability to directly probe the solvent dynamics of a system following resonant electronic excitation on the femtosecond time scale. This technique offers a new perspective for solvation dynamics. The ability to nonresonantly probe the local solvent environment eliminates any reliance on the spectral properties of the solute to report on the dynamic participation of the solvent. This significant advantage will allow the application of this technique to explore a wide range of reactive dynamics in solution, where the reactive event often dominates the spectral properties of the chromophore, typically blinding it as a reporter of the solvent dynamics. By removing the local oscillator from the RaPTOR signal in future applications and leaving the bare $\Delta E^{(3)}(t,\tau)$ response, we believe the evolution of the full spectrum of frequencies, from 0.1 to 500 cm^{-1}, will be available as a function of pump delay t, with time resolution sufficient to follow the fastest events in solution. The ability to identify the coherent participation of the specific solvent frequencies in reactive events should prove valuable in developing models of events such as charge transfer in solution.

Acknowledgment. This work was supported in part by a Camille and Henry Dreyfus New Faculty Award (2000), a nontenured faculty award from 3M (2002), and the MRSEC Program of the National Science Foundation under Award Number DMR-0212302, and acknowledgment is made to the donors of the Petroleum Research Fund, administered by the American Chemical Society, for partial support of this research.

References and Notes

(1) Simon, J. D. *Acc. Chem. Res.* **1988**, *21* (3), 128−134.
(2) Cho, M.; Du, M.; Scherer, N. F.; Fleming, G. R.; Mukamel, S. *J. Chem. Phys.* **1993**, *99* (4), 2410−2428.
(3) Vohringer, P.; Scherer, N. F. *J. Phys. Chem.* **1995**, *99* (9), 2684−2695.
(4) Ruhman, S.; Kohler, B.; Joly, A. G.; Nelson, K. A. *Chem. Phys. Lett.* **1987**, *141* (1−2), 16−24.
(5) Lotshaw, W. T.; McMorrow, D.; Thantu, N.; Melinger, J. S.; Kitchenham, R. *J. Raman Spectrosc.* **1995**, *26*, 571−583.
(6) McMorrow, D.; Thantu, N.; Melinger, J. S.; Kim, S. K.; Lotshaw, W. T. *J. Phys. Chem.* **1996**, *100* (24), 10389−10399.
(7) Joo, T.; Jia, Y.; Yu, J.-Y.; Lang, M. J.; Fleming, G. R. *J. Chem. Phys.* **1996**, *104* (16), 6089−6108.
(8) Fleming, G. R.; Cho, M. H. *Annu. Rev. Phys. Chem.* **1996**, *47*, 109−134.
(9) Horng, M. L.; Gardecki, J. A.; Papazyan, A.; Maroncelli, M. *J. Phys. Chem.* **1995**, *99*, 17311−17337.
(10) Deboeij, W. P.; Pshenichnikov, M. S.; Wiersma, D. A. *Annu. Rev. Phys. Chem.* **1998**, *49*, 99−123.
(11) Hybl, J. D.; Ferro, A. A.; Jonas, D. M. *J. Chem. Phys.* **2001**, *115* (14), 6606−6622.
(12) Barbara, P. F.; Jarzeba, W. *Adv. Photochem.* **1990**, *15*, 1−68.
(13) Jimenez, R.; Fleming, G. R.; Kumar, P. V.; Maroncelli, M. *Nature (London)* **1994**, *369* (6480), 471−473.
(14) Berg, M. A. *J. Phys. Chem. A* **1998**, *102* (1), 17−30.
(15) Berg, M. A. *J. Chem. Phys.* **1999**, *110* (17), 8577−8588.
(16) Larsen, D. S.; Ohta, K.; Fleming, G. R. *J. Chem. Phys.* **1999**, *111* (19), 8970−8979.
(17) Ruhman, S.; Joly, A. G.; Nelson, K. A. *IEEE J. Quantum Electron.* **1988**, *24* (2), 460−469.
(18) Khalil, M.; Demirdöven, N.; Golonzka, O.; Fecko, C. J.; Tokmakoff, A. *J. Phys. Chem. A* **2000**, *104* (24), 5711−5715.
(19) Goodno, G. D.; Dadusc, G.; Miller, R. J. D. *J. Opt. Soc. Am. B* **1998**, *15* (6), 1791−1794.
(20) Maznev, A. A.; Nelson, K. A.; Rogers, A. *Opt. Lett.* **1998**, *23* (16), 1319−1321.
(21) Beard, M. C.; Schmuttenmaer, C. A. *J. Chem. Phys.* **2001**, *114* (7), 2903−2909.
(22) McElroy, R.; Wynne, K. *Phys. Rev. Lett.* **1997**, *79* (16), 3078−3081.
(23) Etchepare, J.; Grillon, G.; Chambaret, J. P.; Hamoniaux, G.; Orszag, A. *Opt. Commun.* **1987**, *63* (5), 329−334.
(24) Hellwarth, R. W. *Prog. Quantum Electron.* **1977**, *5* (Part 1), 1−68.
(25) Berne, B. J.; Pecora, R. P. *Dynamic Light Scattering with Applications to Chemistry, Biology, and Physics*; Wiley: New York, 1976.
(26) Lewis, J. E.; Biswas, R.; Robinson, A. G.; Maroncelli, M. *J. Phys. Chem. B* **2001**, *105* (16), 3306−3318.
(27) Fleming, G. R.; Passino, S. A.; Nagasawa, Y. *Philos. Trans. R. Soc. London, Ser. A* **1998**, *356* (1736), 389−404.
(28) Stratt, R. M.; Maroncelli, M. *J. Phys. Chem.* **1996**, *100* (31), 12981−12996.
(29) Maroncelli, M.; Kumar, V. P.; Papazyan, A. *J. Phys. Chem.* **1993**, *97* (1), 13−17.
(30) Maroncelli, M. *J. Mol. Liq.* **1993**, *57*, 1−37.
(31) Ladanyi, B. M.; Stratt, R. M. *J. Phys. Chem.* **1995**, *99* (9), 2502−2511.
(32) Ladanyi, B. M.; Stratt, R. M. *J. Phys. Chem.* **1996**, *100* (4), 1266−1282.
(33) Backus, S.; Durfee, C. G.; Murnane, M. M.; Kapteyn, H. C. *Rev. Sci. Instrum.* **1998**, *69* (3), 1207−1223.
(34) Ming, L.; Nibarger, J.; Guo, C.; Gibson, G. *Appl. Opt.* **1999**, *38* (24), 5250−5253.
(35) Sweetser, J. N.; Fittinghoff, D. N.; Trebino, R. *Opt. Lett.* **1997**, *22* (8), 519−521.
(36) Suzuki, T.; Nagano, M.; Watanabe, S.; Ichimura, T. *J. Photochem. Photobiol., A* **2000**, *136* (1−2), 7−13.
(37) Ziegler, L. D.; Jordanides, X. J. *Chem. Phys. Lett.* **2002**, *352* (3−4), 270−280.
(38) Mukamel, S. *Principles of Nonlinear Optical Spectroscopy*; Oxford University Press: New York, 1995.
(39) Eesley, G. L.; Levenson, M. D.; Tolles, W. M. *IEEE J. Quantum Electron.* **1978**, *14* (1), 45−49.
(40) Jas, G. S.; Wan, C.; Johnson, C. K. *Appl. Spectrosc.* **1995**, *49* (5), 645−649.
(41) Reynolds, L.; Gardecki, J. A.; Frankland, S. J. V.; Horng, M. L.; Maroncelli, M. *J. Phys. Chem.* **1996**, *100* (24), 10337−10354.
(42) Castner, E. J.; Maroncelli, M. *J. Mol. Liq.* **1998**, *77* (1−3), 1−36.